Tanaka, K., Fujiwara, T., Kumatori, A., Shin, S., Yoshimura, T., Ichihara, A., Tokunaga, F., Aruga, R., Iwanaga, S., Kakizuka, A., & Nakanishi, S. (1990a) *Biochemistry 29*, 3777-3785.

Tanaka, K., Kanayama, H., Tamura, T., Lee, D. H., Kumatori, A., Fujiwara, T., Ichihara, A., Tokunaga, F., Aruga, R., & Iwanaga, S. (1990b) *Biochem. Biophys. Res. Commun. 171*, 676-683.

Tanaka, K., Yoshimura, T., Tamura, T., Fujiwara, T., Kumatori, A., & Ichihara, A. (1990c) *FEBS Lett. 271*, 41-46.

van Riel, M. C. H. M., & Martens, G. J. M. (1991) *FEBS Lett. 291*, 37-40.

Zwickl, P., Pfeifer, G., Lottspeich, F., Kopp, F., Dahlmann, B., & Baumeister, W. (1990) *J. Struct. Biol. 103*, 197-203.

Zwickl, P., Lottspeich, F., Dahlmann, B., & Baumeister, W. (1991) *FEBS Lett. 278*, 217-221.

Articles

Recognition of Tertiary Structure in tRNAs by $Rh(phen)_2phi^{3+}$, a New Reagent for RNA Structure-Function Mapping†

Christine S. Chow,‡ Linda S. Behlen,§ Olke C. Uhlenbeck,§ and Jacqueline K. Barton*,‡

Division of Chemistry and Chemical Engineering, California Institute of Technology, Pasadena, California 91125, and Department of Chemistry and Biochemistry, University of Colorado, Boulder, Colorado 80309

Received September 5, 1991; Revised Manuscript Received October 18, 1991

ABSTRACT: With photoactivation $Rh(phen)_2phi^{3+}$ promotes strand cleavage at sites of tertiary interaction in tRNA. The rhodium complex, which binds double-helical DNA by intercalation in the major groove, yields no cleavage in double-helical regions of the RNA or in unstructured single-stranded regions. Instead, $Rh(phen)_2phi^{3+}$ appears to target regions which are structured so that the major groove is open and accessible for stacking with the complex, as occurs where bases are triply bonded. So as to examine the specificity of this novel reagent and to evaluate its use in probing structural changes in RNAs, cleavage studies have been conducted on two structurally characterized tRNAs, $tRNA^{Phe}$ and $tRNA^{Asp}$ from yeast, the unmodified yeast $tRNA^{Phe}$ transcript, and a chemically modified $tRNA^{Phe}$, as well as on a series of $tRNA^{Phe}$ mutants. On $tRNA^{Phe}$ strong cleavage is observed at residues G22, G45, U47, Ψ55, and U59; weaker cleavage is observed at A44, m^7G46, and C48. On $tRNA^{Asp}$ cleavage is found at residues A21 through G26, Ψ32, and U48, with minor cleavage apparent at A44, G45, A46, Ψ55, U59, and U60. There is a striking similarity in cleavage observed on these tRNAs, and the sites of cleavage mark regions of tertiary folding. Cleavage on the unmodified $tRNA^{Phe}$ transcript resembles closely that found on native yeast $tRNA^{Phe}$, but additional sites, primarily in the anticodon loop and stem, are evident. The results indicate that globally the structures containing or lacking the modified bases appear to be the same; the differences in cleavage observed may reflect a loosening or alteration in the structure due to the absence of the modified bases. Cleavage results on mutants of $tRNA^{Phe}$ illustrate $Rh(phen)_2phi^{3+}$ as a sensitive probe in characterizing tRNA tertiary structure. Results are consistent with other assays for structural or functional changes. Uniquely, $Rh(phen)_2phi^{3+}$ appears to target directly sites of tertiary interaction. Cleavage results on mutants which involve base changes within the triply bonded region of the molecule indicate that it is the structure of the triply bonded array rather than the individual nucleotides which are being targeted. Chemical modification to promote selective depurination of the third base (m^7G46) involved in the triple in the folded, native tRNA leads to the reduction of cleavage by the metal complex; this result shows directly the importance of the stacked triple base structure for recognition by the metal complex. The cleavage results are consistent with the notion that $Rh(phen)_2phi^{3+}$ preferentially targets regions of tertiary structure in the tRNA because these regions are structured so that the major grooves are open and accessible to stacking by the complex. Since sites cleaved by the rhodium complex mark a range of tertiary structures, $Rh(phen)_2phi^{3+}$ appears to be a powerful and unique probe in characterizing the folded structures of RNAs.

Increasing evidence suggests that many of the diverse biological functions of RNA require the molecule to maintain a precise three-dimensional structure (Yanofsky, 1981; Altman, 1984; Cech, 1987; Guerrier-Takada et al., 1989; Rould et al., 1989). A popular approach toward understanding the structure-function relationships of RNA involves extensive site-directed or random mutagenesis of the molecule and assay of the mutants in vitro. In these studies it is important to distinguish whether a decrease in activity of a mutant is the result of a change in an essential nucleotide or the less interesting consequence of a more general alteration of the overall structure. Thus it is important to develop methods to probe rapidly the subtle changes in the configuration of mutant RNA.

† We are grateful to the National Institutes of Health for their financial support. In addition, C.S.C. thanks the Parsons Foundation for their fellowship support.

* To whom correspondence should be addressed.

‡ California Institute of Technology.

§ University of Colorado.

0006-2960/92/0431-972$03.00/0

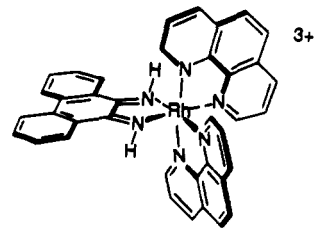

FIGURE 1: Schematic illustration of $Rh(phen)_2phi^{3+}$.

Methods of chemical modification have become increasingly valuable in examining alterations in RNA structure (Ehresmann et al., 1987). Many investigations first demonstrate the utility of chemical agents on the well-characterized transfer RNAs, $tRNA^{Phe}$ (Kim et al., 1974; Quigley & Rich, 1976; Patel et al., 1987) and $tRNA^{Asp}$ (Westhof et al., 1985) from yeast. Different reagents appear to be useful in probing different elements of RNA structure. MPE-Fe(II) (Kean et al., 1985) targets double-helical regions of RNA while $Cu(phen)_2^+$ (Murakawa et al., 1989) appears to mark single-stranded regions. $Ru(phen)_3^{2+}$ (Chow & Barton, 1990), ethylnitrosourea (Romby et al., 1985), and $Fe(EDTA)^{2-}$ (Latham & Cech, 1989; Celander & Cech, 1990) promote strand scission with little or no preference for secondary structure but have the ability to distinguish between protected and exterior regions of the RNA molecule through specific interactions with nucleic acid bases, phosphates, or sugar residues, respectively. Lead-catalyzed cleavage of RNA (Behlen et al., 1990; Werner et al., 1976) depends not upon the presence of a particular secondary structure nor upon solvent accessibility but instead occurs in tRNA with high specificity at a highly structured region of the molecule; hence cleavage with lead ion has been an extremely sensitive assay of structural perturbations local to the Pb^{2+} site.

Transition metal complexes have been designed which target specific nucleic acid sites on the basis of *shape selection* (Pyle & Barton, 1990; Barton, 1986), and these have been useful in mapping variations in local conformation of double-helical DNA (Chow & Barton, 1991; Huber et al., 1991). In particular, bis(phenanthroline)(phenanthrenequinone diimine)-rhodium(III) [$Rh(phen)_2phi^{3+}$] (Figure 1) targets sites which are open in the major groove owing either to propeller twisting or to base tilting (Pyle et al., 1989, 1990). $Rh(phen)_2phi^{3+}$ binds double-helical DNA avidly by intercalation in the major groove and upon photoactivation promotes DNA strand cleavage (Pyle et al., 1989). The cleavage mechanism involves direct abstraction of the C3′ hydrogen atom by the photoactivated metal complex; no diffusible species is involved, and 5′ asymmetric cleavage is observed with a single base stagger, as would be expected with direct attack on the sugar from the major groove by the intercalated complex (Sitlani et al., 1992). The primary cleavage products are 3′- and 5′-phosphate termini and free nucleic acid bases.

The recognition characteristics of $Rh(phen)_2phi^{3+}$ are particularly well suited to probing RNA structure. Double-helical regions of RNA tend to adopt an A-conformation (Arnott et al., 1973; Dock-Bregeon et al., 1989), where the major groove is pulled deeply into the helix interior; as a result the narrowed major groove becomes inaccessible to intercalation. Thus both double-helical regions and unstacked single-stranded regions of an RNA would not be expected to be cleaved by $Rh(phen)_2phi^{3+}$. Cleavage studies using $Rh(phen)_2phi^{3+}$ and other transition metal complexes have been carried out on $tRNA^{Phe}$ (Chow & Barton, 1990). $Rh(phen)_2phi^{3+}$ is unique among the metal complexes in the sites that it targets. Specific recognition by the complex depends upon its shape. The sites targeted by $Rh(phen)_2phi^{3+}$ are neither double helical nor single stranded. The sites also differ from those marked by other structural probes such as lead ion (Behlen et al., 1990) or psoralen (Garrett-Wheeler et al., 1984). Consistent with the recognition characteristics of the rhodium complex on DNA, $Rh(phen)_2phi^{3+}$ targets sites of tertiary interactions in $tRNA^{Phe}$. In particular, $Rh(phen)_2phi^{3+}$ targets triply bonded bases in tRNA, where the third base may provide an accessible surface from the major groove for $Rh(phen)_2phi^{3+}$ stacking.

Here we explore further the efficacy of $Rh(phen)_2phi^{3+}$ using (i) the two tRNAs which have been crystallographically characterized, $tRNA^{Phe}$ (Kim et al., 1974; Quigley & Rich, 1976) and $tRNA^{Asp}$ (Westhof et al., 1985) from yeast, (ii) $tRNA^{Phe}$ containing no base modifications (Sampson & Uhlenbeck, 1988; Hall et al., 1989), (iii) a structurally modified native $tRNA^{Phe}$ (Peattie, 1979), and (iv) a series of $tRNA^{Phe}$ mutants (Sampson et al., 1990). The goals of these efforts have been to delineate the specificity of this reagent and to evaluate the application of the rhodium complex in detecting structural changes in RNA.

Materials and Methods

tRNAs. Unmodified wild-type yeast $tRNA^{Phe}$ and mutants were prepared by in vitro transcription by T7 RNA polymerase (Sampson et al., 1990). Yeast $tRNA^{Asp}$ was a gift from D. Moras. Native yeast $tRNA^{Phe}$ (Boehringer Mannheim), yeast $tRNA^{Asp}$, and the unmodified transcripts were 3′-end-labeled with [5′-^{32}P]pCp (England & Uhlenbeck, 1978) or 5′-end-labeled by dephosphorylation with alkaline phosphatase followed by phosphorylation with [γ-^{32}P]ATP and polynucleotide kinase. The tRNAs were gel purified on a 10% denaturing polyacrylamide gel, located by autoradiography, excised, and eluted from the gel in 45 mM Tris, 45 mM boric acid, and 1.25 mM EDTA, pH 8.0. The eluted tRNAs were ethanol precipitated twice and stored in 10 mM Tris-HCl, pH 8.0.

Cleavage Reactions. $Rh(phen)_2phi^{3+}$ stock solutions were freshly prepared. All end-labeled tRNAs were renatured by heating to 70 °C for 1 min in 10 mM Tris-HCl and 10 mM $MgCl_2$, pH 8.0, and slowly cooling to room temperature prior to use. A typical 20-μL cleavage mixture contained labeled tRNA, 10 μM $Rh(phen)_2phi^{3+}$, and the appropriate buffer (50 mM Tris, 20 mM sodium acetate, 18 mM NaCl, and 1 mM $MgCl_2$, pH 7.0, or 50 mM sodium cacodylate and 1 mM $MgCl_2$, pH 7.0) and was brought to a final concentration of 100 μM in nucleotides with carrier $tRNA^{Phe}$. Irradiation for 10 min at 365 nm at ambient temperature using a 1000-W Hg/Xe lamp and monochrometer yielded site-specific cleavage of the tRNA samples only in the presence of the rhodium complex. The reaction mixtures were ethanol precipitated, washed at least three times with 70% ethanol to remove buffer salts, and analyzed on 15% polyacrylamide–8 M urea gels. The full-length tRNA and cleavage products were identified by coelectrophoresing with diethyl pyrocarbonate (DEPC) (A-specific) and hydrazine (U-specific) reactions (Peattie, 1979) and viewed by autoradiography.

Results

Cleavage of Native Yeast $tRNA^{Phe}$. The sites of $Rh(phen)_2phi^{3+}$ cleavage of native $tRNA^{Phe}$ were determined through cleavage of 5′- and 3′-end-labeled tRNA. The rhodium cleavage sites can be assigned by comparison with end-labeled products of DEPC and hydrazine reactions, which lead to specific cuts at A and U residues, respectively. These base-specific reactions involve the carbethoxylation or alkylation of the RNA bases followed by aniline-catalyzed elimi-

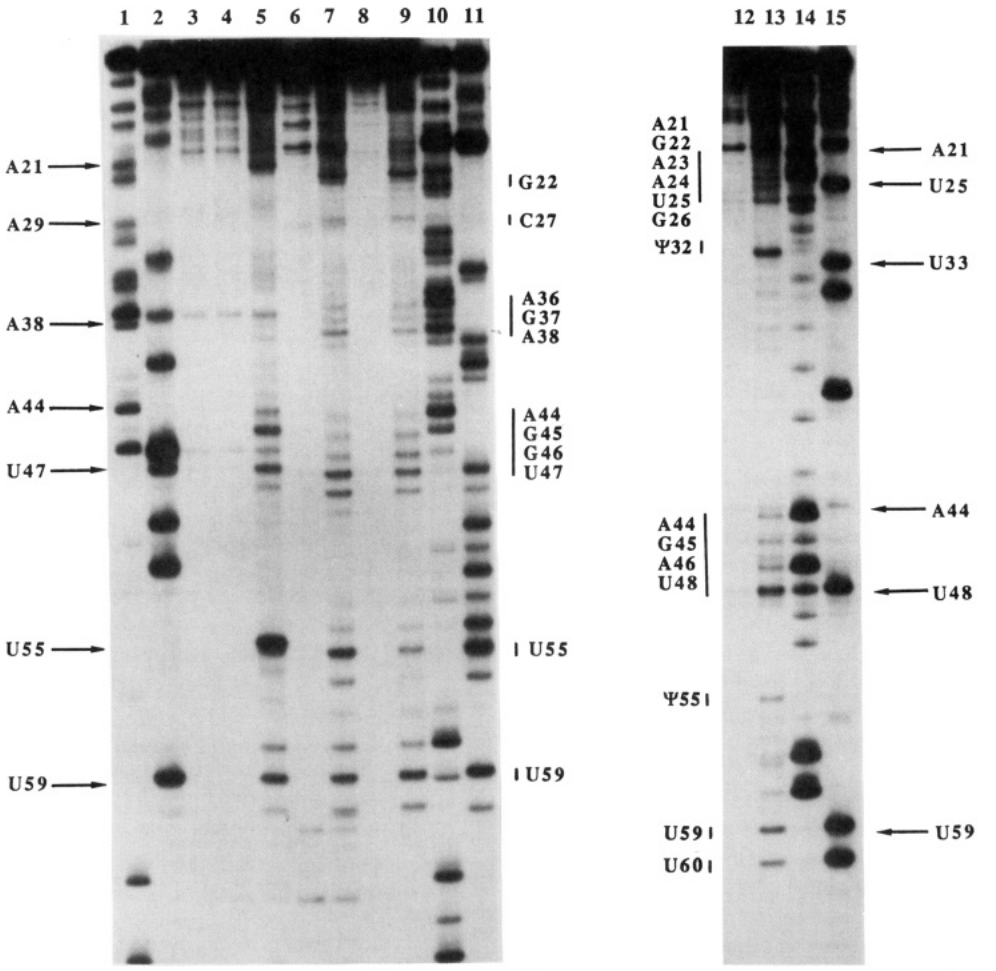

FIGURE 2: Cleavage of ^{32}P 3′-end-labeled native yeast $tRNA^{Phe}$, yeast $tRNA^{Phe}$ transcript, G19C mutant, and yeast $tRNA^{Asp}$ by $Rh(phen)_2phi^{3+}$ in 50 mM Tris, 20 mM sodium acetate, 18 mM NaCl, and 1 mM $MgCl_2$, pH 7.0. Lanes 1, 10, and 14: A-specific reaction on native $tRNA^{Phe}$, $tRNA^{Phe}$ transcript, and $tRNA^{Asp}$. Lanes 2, 11, and 15: U-specific reaction on native $tRNA^{Phe}$, $tRNA^{Phe}$ transcript, and $tRNA^{Asp}$. Lanes 3, 6, 8, and 12 (controls): native $tRNA^{Phe}$, $tRNA^{Phe}$ transcript, G19C, and $tRNA^{Asp}$. Lane 4 (light control): $tRNA^{Phe}$ irradiated in the absence of metal. Lanes 5, 7, 9, and 13: specific cleavage by $Rh(phen)_2phi^{3+}$ on native $tRNA^{Phe}$, $tRNA^{Phe}$ transcript, G19C, and $tRNA^{Asp}$. Arrows indicate reference points along the tRNA sequence. Bars indicate major regions of cleavage of $Rh(phen)_2phi^{3+}$.

nations to give 5′- and 3′-phosphate termini (Peattie, 1979). High-resolution mapping of the rhodium cleavage reactions shows the production of homogeneous 5′- and 3′-termini which comigrate exactly with the phosphate termini generated by DEPC and hydrazine. While the DEPC and hydrazine reactions involve modification of the nucleic acid base and require aniline to facilitate strand scission, the rhodium reactions yield direct strand scission at the ribose. Furthermore, since no diffusible species mediates the reaction, the site of cleavage indicates the site of binding.

As can be seen in Figure 2 (lane 5), few and specific cleavage sites are evident on the 3′-end-labeled tRNA. Strong cleavage occurs at residues G22, G45, U47, Ψ55, and U59. Weaker cleavage is observed at A44, m^7G46, and C48. Identical sites of cleavage are observed in experiments conducted with 5′-end-labeled tRNA with one additional site evident at U8. The U8 site is not observed on the 3′-end-labeled tRNA because of its closeness to the ^{32}P label and the poor resolution of the gels in this region. Also, although most sites produce single 5′- and 3′-termini, cleavage at G22 yields a 5′-phosphate terminus but two 3′-termini. A secondary reaction mechanism which is particular to the geometry of the site may account for the mixture of 3′-termini; to avoid ambiguity in assignment, mapping studies are therefore focused primarily on cleavage of 3′-end-labeled RNAs. These experiments were all conducted under conditions where ≤1 cut per tRNA molecule is obtained. Experiments were also

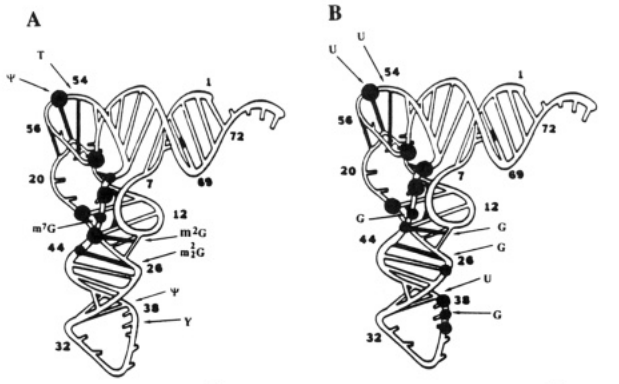

FIGURE 3: $Rh(phen)_2phi^{3+}$ cleavage sites on (A) yeast $tRNA^{Phe}$ and (B) the unmodified $tRNA^{Phe}$ transcript mapped on a ribbon diagram adapted from the crystal structure of $tRNA^{Phe}$ (Kim et al., 1974; Quigley & Rich, 1976). The solid circles indicate the positions of $Rh(phen)_2phi^{3+}$-promoted strand scission with size corresponding to relative cleavage intensity. Arrows indicate the bases which are modified in the native $tRNA^{Phe}$.

conducted at several Rh/RNA ratios and with varying times of irradiation; there were no changes observed in site selectivity.

The ribbon diagram in Figure 3A shows the locations of the major and minor $Rh(phen)_2phi^{3+}$ cleavage sites. These sites are different from those observed using other structure mapping reagents. Figure 4 displays the crystal structure of yeast $tRNA^{Phe}$ with the tertiary interactions highlighted in white

(Figure 4A, left) and the cleavage sites for $Rh(phen)_2phi^{3+}$ in yellow (Figure 4B, left). As can be seen from this figure, cleavage by $Rh(phen)_2phi^{3+}$ occurs predominantly in regions exhibiting extensive tertiary structure. This finding contrasts cleavage studies with other conventional probes which recognize secondary structural features such as double- or single-stranded regions of the tRNA or regions of greater solvent accessibility.

Cleavage at sites which are neither purely single nor purely double stranded may be understood by considering the different structures of an RNA major groove. As shown in Figure 5, an RNA double helix adopts an A-conformation which contains a deep and narrow major groove; the base pairs are pushed out toward the minor groove of the helix. Thus the base pairs are largely inaccessible from the major groove for stacking with the metal complex. No cleavage by $Rh(phen)_2phi^{3+}$ is evident in the double-helical regions of $tRNA^{Phe}$. Three of the eight residues on $tRNA^{Phe}$ (G22, G45, and m^7G46) cleaved by $Rh(phen)_2phi^{3+}$, however, are directly involved in triple interactions in which a third base hydrogen bonds with a normal Watson–Crick base pair in the major groove of the D stem. The interaction of this third base (G45, A9, or G46) in the major groove of the RNA helix creates a structure in which the normally deep and narrow groove is widened and the third base, which fills the groove, is accessible to the helix surface. As shown in Figure 5C, the stacking of these third bases (shown in purple) in the major groove may now provide a platform for stacking with the rhodium complex.

Of the three triples (G45-[m^2G10-C25], A9-[A23-U12], and m^7G46-[G22-C13]), the central A9-[A23-U12] shows no cleavage. This lack of cleavage can be rationalized on the basis of the limited accessibility of the sugar–phosphate backbone in this region. The proposed mechanism of cleavage by $Rh(phen)_2phi^{3+}$ involves direct hydrogen abstraction from the ribose and therefore necessitates that the complex lie close to the sugar in order for a reaction to occur. Residues G45 and m^7G46 are located in the variable loop segment, and their sugars are quite accessible from the major groove side of the D stem (phosphates of this strand are in yellow in Figure 5). Residue A9 comes from another segment of the polynucleotide chain and intercalates between G45 and m^7G46 with its backbone buried within the molecule (phosphates of this strand are in orange); as seen in Figure 5, although stacking with the metal complex is feasible, the sugar residues of this strand are not accessible from the major groove side for cleavage.

The strong cleavage by $Rh(phen)_2phi^{3+}$ apparent at the TΨC loop residues Ψ55 and U59 is not as well understood. As is evident from the crystal structure, this region contains extensive tertiary interactions, and these unusual base interactions between the D and TΨC loops (G18-Ψ55, G19-C56) may provide a structure which facilitates the interaction with the rhodium complex. Cleavage at U59 is also difficult to understand. This residue is not base paired, however, it lies stacked in the core region of the molecule. It is unclear whether the U59 site is uniquely recognized by $Rh(phen)_2phi^{3+}$ or if cleavage here is a result of stacking interactions with the neighboring triply bonded sites.

Effect of Salt Variation on $tRNA^{Phe}$ Cleavage. Cleavage by the rhodium complex varies as a function of magnesium and sodium concentrations and buffer conditions. The original cleavage experiments were performed in sodium acetate buffer (50 mM Tris, 20 mM sodium acetate, 18 mM NaCl, 1 mM $MgCl_2$, pH 7.0). In 50 mM sodium cacodylate and 1 mM $MgCl_2$, pH 7.0, additional cleavage sites are observed at residues Y37, A38, and Ψ39 in the anticodon loop. There is also diminished cleavage at U47. However, with increasing concentrations of NaCl (up to 75 mM) a loss in cleavage at the anticodon residues is observed, and increased cleavage at U47 is apparent with no change at the other sites. Similarly, a loss of cleavage in the anticodon loop residues is associated with added $MgCl_2$ (0.5–10 mM) as is a loss in cleavage at the triple base sites. Cleavage at Ψ55 and U59 appears to be independent of magnesium and salt concentrations. Apparently the particular orientation of the D and TΨC loops required for recognition by $Rh(phen)_2phi^{3+}$ is not altered in the presence of up to 10 mM $MgCl_2$ or 75 mM NaCl.

These results suggest that with increasing magnesium concentrations the conformational changes in the tRNA are localized. The overall structure of the tRNA is likely to be unchanged, but a local loosening or tightening of the structure may occur, which is detected by $Rh(phen)_2phi^{3+}$. For example, it has been shown through fluorescence studies on the Y base that the presence of magnesium ion causes the anticodon loop to be more structured (Beardsley et al., 1970) but has little effect on the overall shape of the molecule. The loss of cleavage in the anticodon loop and at the triple base sites may be associated with a tightening of the structure. Alternatively, but unlikely on the basis of relative affinities, the magnesium ion may simply be competing with the rhodium complex for binding at these sites.

Cleavage of Yeast $tRNA^{Asp}$. On the basis of its crystal structure (Westhof et al., 1985), the tertiary structure of yeast $tRNA^{Asp}$ resembles that of $tRNA^{Phe}$ (Figure 4A). Therefore, in order to define further the recognition by $Rh(phen)_2phi^{3+}$, we have examined cleavage by $Rh(phen)_2phi^{3+}$ on yeast $tRNA^{Asp}$. There is a striking similarity in cleavage patterns observed on yeast $tRNA^{Phe}$ and $tRNA^{Asp}$ (Figure 4B). Strong cleavage, as shown in Figure 2 (lane 13), is observed at residues A21 through G26, Ψ32, and U48, with minor cleavage apparent at A44, G45, A46, Ψ55, U59, and U60. Again, the sites of cleavage appear to mark regions of tertiary folding of the tRNA molecule, as compared in Figure 4 (panels A and B, right).

Five of the 14 sites in $tRNA^{Asp}$ which are cleaved by $Rh(phen)_2phi^{3+}$ are directly involved in triple base interactions and three neighbor and stack with the base triples. The remaining cleavage sites are located in the anticodon and TΨC loops. The tertiary interactions found in yeast $tRNA^{Asp}$ are generally analogous to those observed in yeast $tRNA^{Phe}$, but with some minor differences which may affect cleavage. Most of the differences in cleavage between $tRNA^{Asp}$ and $tRNA^{Phe}$ can be explained by the crystal structure data.

Let us first consider the sites of triple base interaction. The following interactions occur in the major groove of the D stem: G45-[G10-U25], A9-[A23-U12], and A46-[G22-Ψ13]. It appears that the presence of only four bases (A44, G45, A46, U48) in the variable loop of yeast $tRNA^{Asp}$ as compared to five (A44, G45, G46, U47, C48) in yeast $tRNA^{Phe}$ induces a different stacking environment for the base triples, as is revealed when the crystal structures are compared (panels B and C of Figure 5). The base triples in $tRNA^{Asp}$ are more evenly stacked on one another compared to the base triples in $tRNA^{Phe}$. The presence of G-U mismatched base pairs may also contribute to the increased stacking of the base triples in $tRNA^{Asp}$ (Westhof et al., 1985). There is a greater uniformity in cleavage observed across the triple sites in $tRNA^{Asp}$ as compared with $tRNA^{Phe}$; this uniformity may be a function of the evenness or columnar stacking apparent in the triply bonded region of $tRNA^{Asp}$.

Another structural difference apparent in $tRNA^{Asp}$ is a

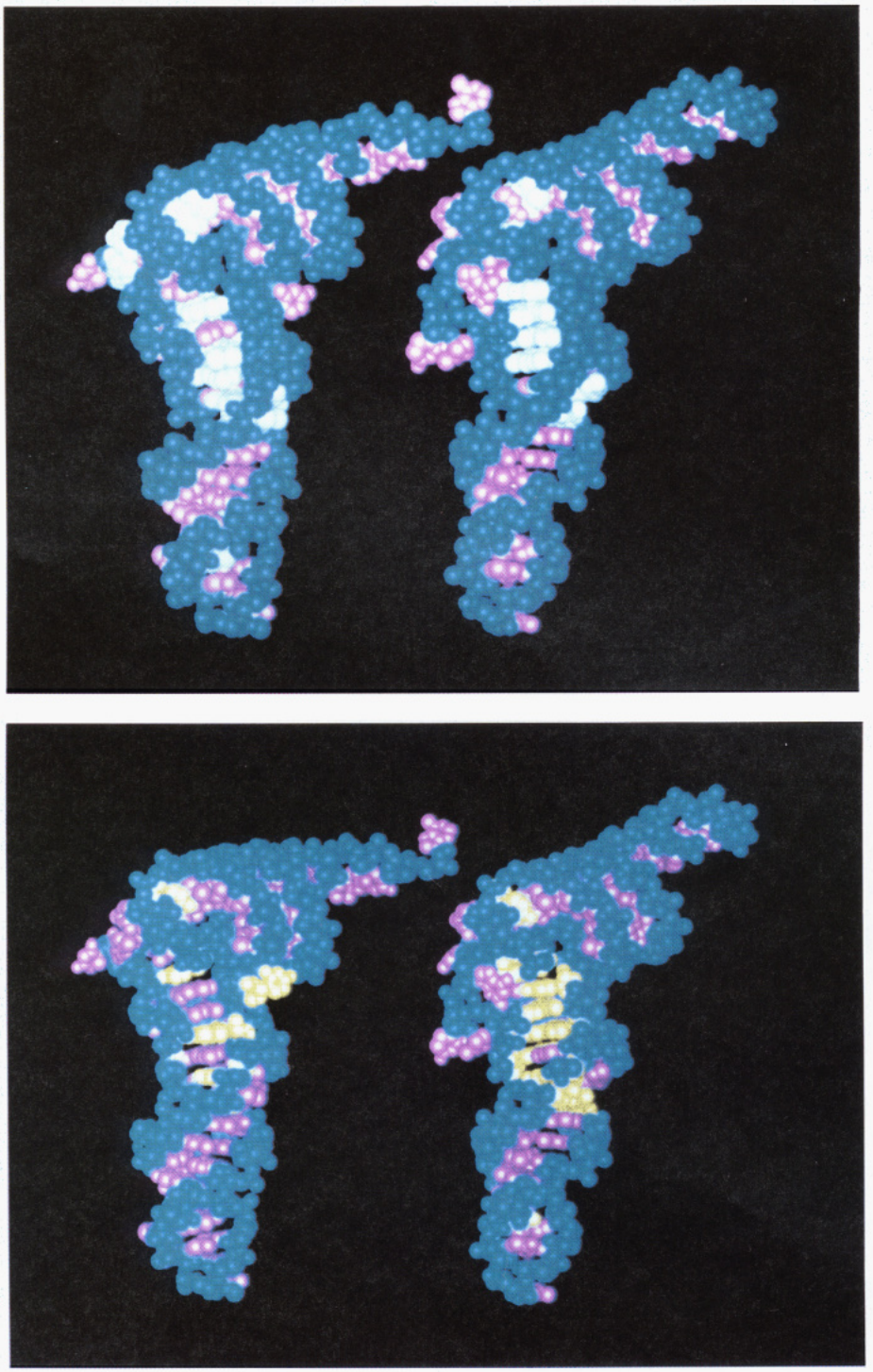

FIGURE 4: Tertiary interactions and cleavage data for $Rh(phen)_2phi^{3+}$ shown in a computer graphic representation of the crystal structures of yeast $tRNA^{Phe}$ and $tRNA^{Asp}$. The sugar–phosphate backbones are shown in aqua and the nucleic acid bases in purple. (A, top) The bases involved in tertiary interactions are shown in white for $tRNA^{Phe}$ (left) and $tRNA^{Asp}$ (right). (B, bottom) The residues (bases and sugars) which are cleaved by $Rh(phen)_2phi^{3+}$ are shown in yellow for $tRNA^{Phe}$ (left) and $tRNA^{Asp}$ (right). Note the correspondence between the white and yellow regions where $Rh(phen)_2phi^{3+}$ promotes strand scission.

rotation of the A15-U48 Levitt pair with respect to U8-A14. This rotation leads to an interaction of A21 with the sugar of U8 and base of A14 to form a fourth base triple; A21 of $tRNA^{Phe}$ interacts only with the sugar of U8. Ethylnitrosourea alkylation studies (Romby et al., 1985) have revealed the differential reactivities of phosphates in the two tRNA species. Phosphate 22 in the D stem is protected in $tRNA^{Asp}$, yet accessible in $tRNA^{Phe}$. In contrast, phosphates 23 and 24 are accessible in $tRNA^{Asp}$, but partially protected in $tRNA^{Phe}$. Our results show that sugar residue 22 is most accessible in $tRNA^{Phe}$, while residues 23, 24, and neighboring residues are accessible in $tRNA^{Asp}$. We have also observed strong cleavage at position 48 on $tRNA^{Asp}$, but not $tRNA^{Phe}$. This may also be a result of the different conformation of the neighboring U8-A14-A21 triple interaction. Again, Figure 5B shows the more evenly stacked arrangement for A21 and U48 in $tRNA^{Asp}$.

The crystal structure of $tRNA^{Asp}$ reveals the absence of G19-C56 base pairing and other interactions between the D and TΨC loops typical of $tRNA^{Phe}$. Cleavage by $Rh(phen)_2phi^{3+}$ is apparent at the TΨC loop residues Ψ55, U59, and U60 on the $tRNA^{Asp}$, but the cleavage associated with

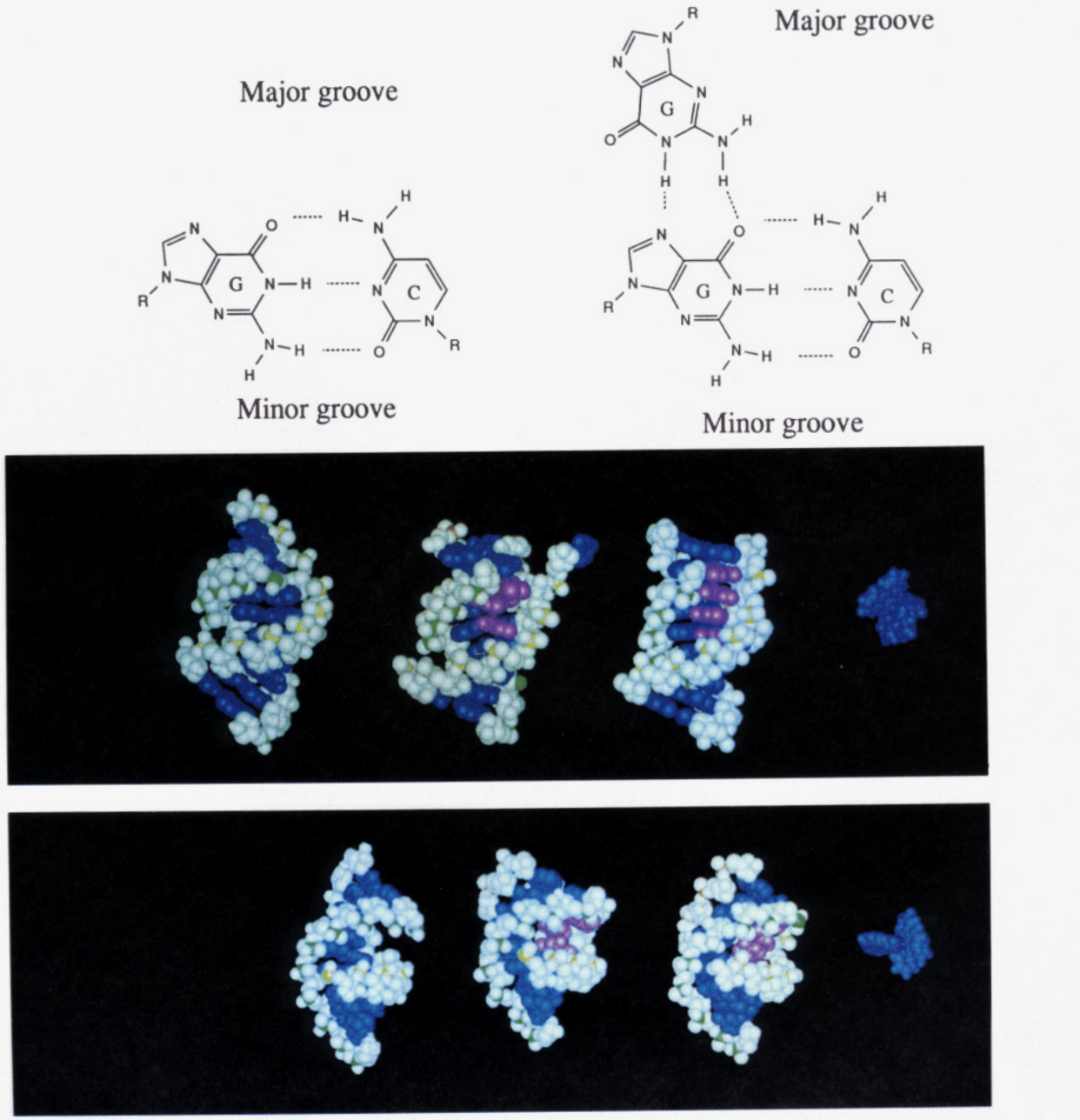

FIGURE 5: Illustrations of the basis for recognition of the triply bonded bases by $Rh(phen)_2phi^{3+}$. (A, top) Structure of a G-C base pair and a G-[G-C] triple base pair. (B, middle) Comparison of an A-form RNA double helix (left) and two triple helix regions based on the crystal structures of yeast $tRNA^{Phe}$ (middle) and $tRNA^{Asp}$ (right). Bases are blue; phosphorus atoms are yellow for strand 1, green for strand 2, and orange for strand 3; the third bases interacting in the major groove are shown in purple (from top to bottom, G45, A9, and G46 for $tRNA^{Phe}$ and A21, G45, A9, and A46 for $tRNA^{Asp}$); all other atoms are white. For comparison of sizes, the rhodium complex is shown in blue to the far right. Note that the sugar residues of G45 and G46 are accessible from the major groove (yellow strand), while the sugar of A9 is buried within the molecule (orange strand). The view in (B) is perpendicular to the helix axis. The helices in (C, bottom) have been rotated 90° and tilted approximately 45° to afford a view into the major groove. Note how the third bases fill the major groove of an A-like helix and are accessible for stacking from the major groove with the metal complex.

this region is much weaker than that observed on $tRNA^{Phe}$. In the $tRNA^{Asp}$ crystal (Westhof et al., 1985), C56 remains stacked on G57; however, G19 is displaced by about 4 Å compared to $tRNA^{Phe}$. As a consequence, the G19-C56 base pair, which is important for maintenance of the D–TΨC loop interactions in $tRNA^{Phe}$, is disrupted. Solution studies on $tRNA^{Asp}$, however, revealed protection from N-3 alkylation by dimethyl sulfate at C56, which according to the crystal structure should be reactive (Romby et al., 1987). The lack of reactivity of C56 suggested the existence of a G19-C56 Watson–Crick base pair correlated with the free state of the molecule in solution. Our results indicate that the rhodium complex is still recognizing structure in the TΨC loop, but to a lesser extent than observed for $tRNA^{Phe}$. Perhaps this region in the $tRNA^{Asp}$ is structured somewhat like $tRNA^{Phe}$, but with more flexibility.

Other differences in cleavage by $Rh(phen)_2phi^{3+}$ on $tRNA^{Asp}$ and $tRNA^{Phe}$ are seen in the anticodon loops. On $tRNA^{Phe}$, we see cleavage of the anticodon residues Y37, A38, and Ψ39 only under certain salt conditions, whereas on $tRNA^{Asp}$, we see strong cleavage at Ψ32. This is consistent with the data of Romby et al. (1987), who showed that the loop residues of $tRNA^{Asp}$ are more susceptible to chemical modification under native conditions than of $tRNA^{Phe}$, suggesting that the anticodon loop in $tRNA^{Asp}$ is structurally different. This could result from the different stacking interactions in $tRNA^{Asp}$ because of the long-range effects such as the G30-U40 mismatched base pair in the anticodon stem

Table I: Cleavage of $tRNA^{Phe}$ Mutants by $Rh(phen)_2phi^{3+}$ Compared with Lead Cleavage Rates and Aminoacylation Kinetics

mutant	tertiary interaction[a]	diminished sites[b]	enhanced sites[b]	Pb[c]	aminoacylation[d]
wild type	G19-C56, G18-U55			(1.0)	(1.0)
G19C	**C19**-C56	48, 55	45, 46	ND[e]	ND
G18A-U55C	**A18-C55**		54, 55	0.42	0.23
wild type	G46-[G22-C13]			(1.0)	(1.0)
G46C	**C46**-[G22-C13]	lose 45, 47, 48, 55		0.22	0.40
G22A-C13U	G46-[**A22-U13**]		45, 46	0.40	0.53
G46A-G22A-C13U	**A46**-[**A22-U13**]	48	44, 45, 46	0.44	1.20
wild type	A9-[A23-U12]			(1.0)	(1.0)
A9U	**U9**-[A23-U12]	36, 37, 38, 46, 47, 59		0.18	0.55
wild type	G45-[G10-C25]			(1.0)	(1.0)
G45U	**U45**-[G10-C25]		45, 46, 47	0.87	0.95
G10C-C25G	G45-[**C10-G25**]	27, 36, 37, 38, 48	45, 46, 54, 55, 60	ND	0.88

[a] Tertiary interactions for wild type are in regular type and mutations are in bold type. [b] Cleavage relative to wild-type $tRNA^{Phe}$ transcript. Cleavage mixtures contained 3′-end-labeled tRNA, 10 μM $Rh(phen)_2phi^{3+}$, 100 μM carrier $tRNA^{Phe}$, 50 mM Tris, 20 mM sodium acetate, 18 mM NaCl, and 1 mM $MgCl_2$, pH 7.0 at 25 °C. [c] Taken from Behlen et al. (1990). [d] Taken from Sampson et al. (1990). [e] ND, not detected.

or different base composition in the loop itself.

The effects of magnesium ion on cleavage of $tRNA^{Asp}$ also differ from those seen on $tRNA^{Phe}$. However, the results on $tRNA^{Asp}$ are consistent with the notion of only localized conformational changes in the tRNA in the presence of magnesium ions. A loss of cleavage is observed at the triple base sites in 10 mM $MgCl_2$, consistent with a tightening of the structure in this region so as to inhibit interactions with $Rh(phen)_2phi^{3+}$. In contrast to the $tRNA^{Phe}$ results, increased cleavage is observed in the TΨC loop residues in $tRNA^{Asp}$. In the case of the TΨC loop, a magnesium-induced structural change may actually enhance interaction with the rhodium complex. No change in cleavage at the anticodon residues Ψ32 is associated with increased magnesium ion. Unlike on $tRNA^{Phe}$, Mg^{2+} seems to have little effect on the structure of the anticodon loop in $tRNA^{Asp}$ and subsequent interaction with $Rh(phen)_2phi^{3+}$.

Cleavage of Unmodified tRNA. Cleavage by $Rh(phen)_2phi^{3+}$ of the yeast $tRNA^{Phe}$ transcript, which lacks all 14 modified nucleotides but otherwise contains no base substitutions, was also examined. Thermal melting profiles of the transcript show that, at low magnesium concentrations, the transcript possesses a less stable structure as compared to the native yeast $tRNA^{Phe}$ (Sampson & Uhlenbeck, 1988); even in high magnesium concentrations (8 mM), the transcript exhibits a different melting profile, suggesting a more flexible structure than the fully modified yeast $tRNA^{Phe}$. Perhaps the absence of specific base modifications causes an overall destabilization of the tRNA transcript. NMR studies on the $tRNA^{Phe}$ transcript have also indicated that even when the transcript is folded normally (5 mM free $MgCl_2$), local structural changes may arise because of the absence of base modifications (Hall et al., 1989).

Cleavage of unmodified $tRNA^{Phe}$ by $Rh(phen)_2phi^{3+}$ seems to be similar but not identical to that of fully modified $tRNA^{Phe}$. Strong cleavage, shown in Figure 2, is apparent at G22, U47, C48, U55 (Ψ55 in native), and U59 with minor sites at C27, A36, G37 (Y37 in native), A38, G45, and G46 (m^7G46 in native). The rhodium cleavage results therefore indicate that globally the folded structure of the tRNA is likely the same. Furthermore, the fact that the sites of cleavage are in general the same on the modified and unmodified tRNAs also provides evidence that the complex is recognizing a specific shape or structure and that the actual cleavage chemistry is not related to the base modifications.

The differences in cleavage between native and wild-type $tRNA^{Phe}$ are shown in a ribbon diagram in Figure 3. Changes in cleavage in the anticodon loop (residues 36–38) and the anticodon stem (residue 27) may reflect a loosening or alteration in the structure due to the absence of the modified bases. In contrast to modified native $tRNA^{Phe}$, cleavage of the anticodon loop residues in the unmodified tRNA transcript is actually enhanced in 10 mM $MgCl_2$. This may be reflective of the subtle structural differences between the modified and unmodified RNA rather than blocking effects of the bulky modified base. A decrease in cleavage at U55 may also reflect the absence of modified bases at residues 54 and 55. Similarly, the small changes in selectivity by the rhodium complex in the triple base region could be a result of minor structural variations which arise when modified bases are no longer present to stabilize specific interactions. For example, the hydrogen bonding at the m^7G46-[G22-C13] triple by N_1 and the exocyclic N_2 of G46 may be stabilized by the increased positive charge associated with methylation at N_7. The positive charge may also stabilize the interactions of G46 with phosphate 9. The triple G45-[m^2G10-C25] is followed by the severely propeller twisted A44-m^2_2G26 base pair. The m^2G10-C25 base pair stacks with m^2_2G26, while A44 stacks with the C27-G43 pair below. The dimethylation of G26 may contribute to the propeller twisting of the base pair and therefore stabilize the stacking interaction at the neighboring triple site. These interactions are likely important for recognition by the rhodium complex as seen by changes in cleavage at A44, G45, and G46, as well as C27. Also, similar to native $tRNA^{Phe}$, a gradual loss in cleavage at G22, U47, and C48 with increasing magnesium is observed. With increasing magnesium ion concentrations, no cleavage is apparent at A44, G45, and G46, however, suggesting that the unmodified tRNA transcript may be structurally slightly different from native tRNA, even in the presence of magnesium, rather than simply more flexible.

Cleavage of tRNA Mutants. In order to characterize further the recognition characteristics of the rhodium complex, cleavage was examined on a series of mutant tRNAs prepared as RNA transcripts. Table I summarizes the findings obtained. Table I also shows comparison of the rhodium cleavage data to assays of mutant structure based upon cleavage by lead ion (Behlen et al., 1990) and rates of aminoacylation (Sampson et al., 1990). In this fashion the use of rhodium cleavage as an assay for RNA structural perturbations may be compared and contrasted to current methodologies.

Mutations of Tertiary Interactions in the D–TΨC Loop Region. We were interested in exploring how changes in the D–TΨC loop interactions might perturb the overall tertiary structure of the RNA. Figure 6 summarizes the cleavage data for two different D–TΨC loop mutants. These mutations occur at neighboring residues and have substantially different

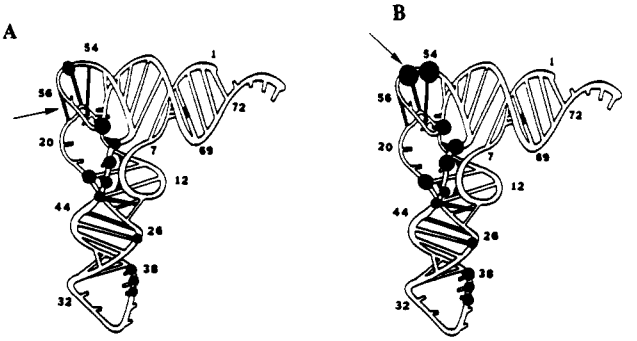

FIGURE 6: Mapped sites of cleavage on the TΨC loop mutants (A) G19C and (B) G18A-U55C. Arrows point to the sites of mutation.

effects on the TΨC loop cleavage. These effects are localized, however, and little change in cleavage is observed at the triple base or anticodon sites.

The crystal structure of yeast $tRNA^{Phe}$ shows that the nucleotides G19-C56 form the only tertiary Watson–Crick base pair in the outermost corner of the tRNA molecule and are important for maintaining interactions between the D and TΨC loops. The G19C mutant leads to a C19-C56 mismatch which is expected to partially disrupt the D–TΨC loop interaction. An observed 5-fold decrease in the rate of site-specific cleavage by lead indicates that this mutant has an altered tertiary structure in the corner region of the $tRNA^{Phe}$ molecule (Behlen et al., 1990). $Rh(phen)_2phi^{3+}$ promotes strand scission of G19C (Figure 2) at U59 and the anticodon residues to the same extent as in the wild-type transcript, but there are small changes in cleavage at the triple base sites and a noticeable decrease in cleavage at U55. This result is consistent with cleavage results on yeast $tRNA^{Asp}$; the disrupted G19-C56 base pair evident in the crystal structure seems to have only small long-range effects on cleavage by $Rh(phen)_2phi^{3+}$ at the triple base sites, but less cleavage at the U55 site with less selectivity is apparent.

The mutant G18A-Ψ55C (data not shown) shows overall patterns of cleavage by $Rh(phen)_2phi^{3+}$ which are similar to wild type, but with greatly enhanced cleavage at U54 and C55. This mutation is expected to have significant effects on the interaction between the D and TΨC loops. The aminoacylation kinetics of this mutant indicate that the hydrogen-bonding interactions between G18 and Ψ55 are important for interaction with the cognate yeast phenylalanyl-tRNA synthetase (Table I). In addition, decreased lead cleavage suggests that this mutant has an altered tertiary structure. Our data suggest that the tRNA is still folded with its overall structure the same, but a significant structural change has occurred in the D–TΨC loop region. Together with the $tRNA^{Asp}$ cleavage data, these results point to the importance of the TΨC loop structure for the recognition by the rhodium complex.

Mutations of the G46-[G22-C13] Tertiary Interaction. In the core region of the tRNA molecule, the G22-C13 base pair in the D stem interacts with G46 of the variable loop. This triple base scheme is stabilized by seven hydrogen bonds (four tertiary) in $tRNA^{Phe}$ and three hydrogen bonds (one tertiary) in $tRNA^{Asp}$. Mutations in this tertiary interaction were constructed to maintain the conserved Py13-Pu22 motif and vary at position 46. These mutations exhibit relatively small differences in aminoacylation kinetics and only slight reductions in lead cleavage (Table I). Importantly, $Rh(phen)_2phi^{3+}$ targets the same sites in these mutants, which verifies that the complex recognizes structural features of the RNA rather than individual nucleotides.

Not only does the rhodium complex target the triple base structure in tRNA, but $Rh(phen)_2phi^{3+}$ is also able to distinguish small variations in the backbone structure around the base triples. As shown in Figure 7 (lane 7), a one-base change to **C46**-[G22-C13] leads to a large change in cleavage at G45 through C48. This mutant appears unstable since the overall cleavage is much weaker and less specific at both the triple sites and the D loop sites. A relative lead cleavage of 0.22 compared to wild-type cleavage is also indicative of some structural change for this mutation (Behlen et al., 1990).

We have also examined a two-base change at the D stem base pair to G46-[**A22-U13**] and a three-base change to **A46**-[**A22-U13**], a common base triple found among tRNAs. Figure 7 (lanes 9 and 11) shows cleavage patterns similar to those on the wild-type transcript, but with strong cleavage at G46 for both mutants. These data are also compared in Figure 8 (A and B). Changes in cleavage at the triple base sites for these mutants may be understood by considering variations in the base-stacking interactions. As was evident also in the $tRNA^{Asp}$ cleavage data, the rhodium complex is sensitive to variations in base stacking of the triples, as would be expected if the rhodium complex intercalates in this region. Perhaps the greater change in cleavage in **C46**-[G22-C13] results from a greater change in stacking, since the mutation involves a purine to pyrimidine base change at residue 46. Mutants G46-[**A22-U13**] and **A46**-[**A22-U13**], on the other hand, involve only semiconservative base changes. The conservation of a purine at position 22 and a pyrimidine at position 13 may help to maintain proper stacking interactions within these triple base regions. Not surprisingly with an intercalator, the stacking may actually be more important than hydrogen-bonding interactions among bases in determining the interactions with $Rh(phen)_2phi^{3+}$.

Mutations of the A9-[A23-U12] Tertiary Interaction. A reverse Hoogsteen pair with A9 occurs in the major groove of the A23-U12 base pair of the D stem. This triple is flanked by two other triples (G46-[G22-C13] and G45-[G10-C25]), and the A9 residue is stabilized by stacking interactions with the G45 and G46 residues. The mutant which involves a one-base change of the third base **U9**-[A23-U12] exhibits only small changes in the cleavage patterns, as shown in Figure 7 (lane 13). We have observed a small decrease in $Rh(phen)_2phi^{3+}$ cleavage at all sites except U55 but a large decrease in the lead cleavage rate (0.18) (Table I). This mutant maintains only one hydrogen bond between U9 and A23; however, the triple may be stacked such that it is still recognized by the rhodium complex.

Mutations of the G45-[G10-C25] Tertiary Interaction. The crystal structure of $tRNA^{Phe}$ shows that the variable loop nucleotide G45 has a single hydrogen bond between its exocyclic amine and the O_6 of G10 in the major groove of the D stem and that G45 is tilted and stacked over A44. Furthermore, A44 stacks with the first base of the anticodon stem, while the G10-C25 base pair stacks over G26. The propeller-twisted A44-G26 base pair maximizes stacking with its neighboring nucleotides. The mutations G45U and G10C-C25G, which should form the base triples **U45**-[G10-C25] and G45-[**C10-G25**], respectively, exhibit normal aminoacylation kinetics compared with wild type but, as seen in Table I, show very different rates of cleavage with lead. As with the other triple base mutants, the overall patterns of cleavage by $Rh(phen)_2phi^{3+}$ are the same as wild type (Figure 7, lanes 15 and 17, illustrated in Figure 8C,D), again supporting the notion that the rhodium complex recognizes the triple base structure rather than individual nucleotides. One can, however, observe

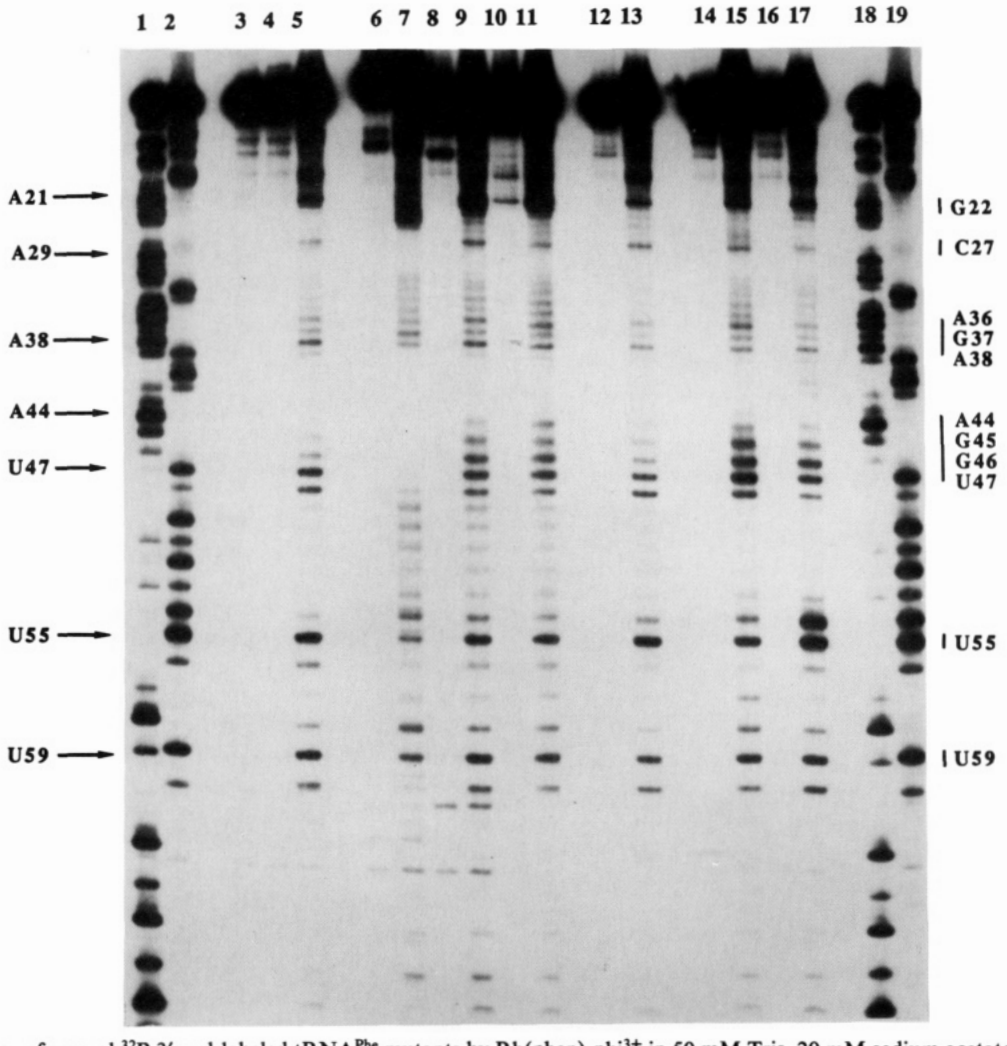

FIGURE 7: Cleavage of several ^{32}P 3′-end-labeled $tRNA^{Phe}$ mutants by $Rh(phen)_2phi^{3+}$ in 50 mM Tris, 20 mM sodium acetate, 18 mM NaCl, and 1 mM $MgCl_2$, pH 7.0. Lanes 1 and 18: A-specific reaction on the $tRNA^{Phe}$ transcript. Lanes 2 and 19: U-specific reaction on the $tRNA^{Phe}$ transcript. Lanes 3, 6, 8, 10, 12, 14, and 16 (controls without metal or irradiation): $tRNA^{Phe}$ transcript, G46C, G22A-C13U, G46A-G22A-C13U, A9U, G45U, and G10C-C25G. Lane 4 (light control): $tRNA^{Phe}$ transcript irradiated in the absence of metal. Lanes 5, 7, 9, 11, 13, 15, and 17: specific cleavage by $Rh(phen)_2phi^{3+}$ on the $tRNA^{Phe}$ transcript, G46C, G22A-C13U, G46A-G22A-C13U, A9U, G45U, and G10C-C25G. Arrows indicate reference points along the tRNA sequence. Bars indicate major regions of cleavage by $Rh(phen)_2phi^{3+}$.

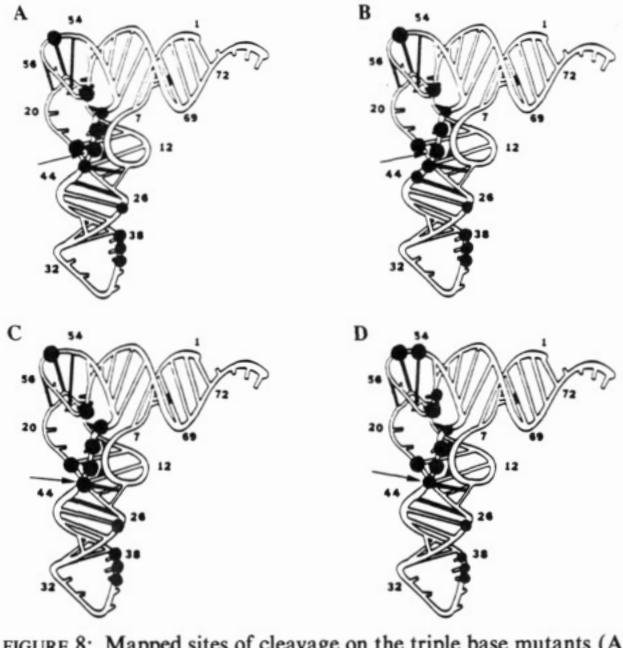

FIGURE 8: Mapped sites of cleavage on the triple base mutants (A) G22A-C13U, (B) G46A-G22A-C13U, (C) G45U, and (D) G10C-C25G. Arrows point to the sites of mutation.

differences within these regions of cleavage. Cleavage at A44, U45, and G46 on G45U is unusually strong compared to cleavage on the wild-type transcript. Once again, stacking interactions may be more important than hydrogen-bonding interactions in determining binding by the rhodium complex. Hydrogen bonding between G10 and U45 is unlikely, but it seems that the presence of residue 45 in the major groove of the D stem is sufficient for recognition by the rhodium complex. The presence of the two neighboring triple sites may also help to maintain stacking in this mutant, although stacking of a pyrimidine (U45) is less favored than stacking of a purine (G45).

The G10C-C25G mutant shows small changes in cleavage at the triple sites and a diminished intensity of cleavage in the anticodon loop and at residue C27. These variations may indicate a more global change in structure of the mutant. Unusually strong cleavage is evident in the D–TΨC loop region. Consistent with the rhodium cleavage data, this mutation showed a pronounced effect on the lead cleavage at a site far from the mutation (Behlen et al., 1990).

Removal of the m^7G46 Residue in Native $tRNA^{Phe}$. Chemical modification in which a triple base interaction is destroyed without substantial effect elsewhere in the molecule is also useful in delineating the recognition of the triple base

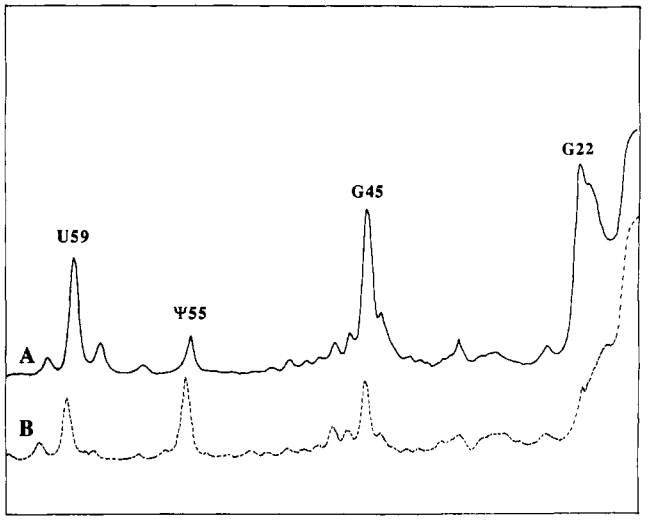

FIGURE 9: Densitometer scans of Rh(phen)$_2$phi^{3+} cleavage of (A) native tRNA^{Phe} and (B) the chemically modified tRNA^{Phe}. Cleavage reactions were performed in 50 mM sodium cacodylate, pH 7.0. The native tRNA^{Phe} was modified with sodium borohydride as described by Peattie (1979) prior to cleavage by the metal complex. The major sites of cleavage are marked.

sites by Rh(phen)$_2$phi^{3+}. Upon sodium borohydride treatment of the native tRNA^{Phe}, residue G46, which is methylated at the N7 position, is depurinated (Peattie, 1979). This depurination leads to a loss of the third base interaction in the major groove for the triple G46-[G22-C13]. As shown in Figure 9, the cleavage by Rh(phen)$_2$phi^{3+} on the still intact, folded, depurinated tRNA indicates a large reduction in the cleavage intensity at the triple sites (G45 and G22) and neighboring site (U59) relative to the other sites of cleavage (Ψ55) which are far from the mutation. It is difficult to bring both the borohydride reduction and aniline treatment to completion, however, to permit quantitation of the effect. Additionally, other base modifications, such as depurination at Y37, may occur, which may also cause structural perturbations in the tRNA. Nonetheless, with these caveats, it appears that the triply bonded base in the folded tRNA is essential for recognition by the rhodium complex.

Discussion

We have shown that Rh(phen)$_2$phi^{3+} is a sensitive probe of the tertiary structure of tRNAs. There is a strong correlation evident between regions of the RNA which are involved in tertiary interactions and sites which are specifically targeted by the rhodium complex. The sites differ from those targeted by other cationic metal complexes which differ in their shape. Mutations which preserve the structure of the triply bonded region of the tRNA are still cleaved by Rh(phen)$_2$phi^{3+}, indicating that it is the structure rather than the individual nucleotides which are being targeted. Selective depurination of m^{7}G46, the third base involved in the triple in the native, folded tRNA, results in the reduction of cleavage by the metal complex. These results are consistent with the DNA recognition characteristics of Rh(phen)$_2$phi^{3+}. While the complex binds by an intercalative mode in the major groove of DNA, binding by the complex in the deep and narrow major groove of double-helical RNA is not expected on the basis of steric considerations. Indeed, no cleavage is observed in double-helical regions of tRNA. Additionally, the complex requires structure in order to intercalate, and thus purely single-stranded regions of the RNA are not targeted by the complex. Furthermore, since the complex cleaves by direct hydrogen abstraction, rather than through a diffusible intermediate, close contact with the RNA is required to achieve strand scission. *We therefore propose that cleavage by Rh(phen)$_2$phi^{3+} preferentially occurs at regions of tertiary structure in the tRNA because these regions are structured so that the major grooves are open and accessible to stacking by the complex.*

The rhodium complex is not, however, specific for one particular tertiary structure. Instead, on the basis of cleavage results for yeast tRNA^{Phe}, yeast tRNA^{Asp}, and the structurally modified tRNA mutants, it appears that a variety of tertiary structures are recognized by Rh(phen)$_2$phi^{3+}. These structures include triple base interactions, stem–loop junctions such as in the anticodon stem–loop region, or the structured loop regions such as the TΨC loop. Furthermore, as can be seen in Table I, the rhodium complex provides a sensitive probe for structural perturbations within these regions. One or two base changes can affect cleavage at neighboring residues which may be a result of different base-stacking interactions for purines versus pyrimidines (i.e., G45U) or local structural distortions created by altered hydrogen-bonding interactions between the bases (G18A-U55C). As is also evident from Table I, mutations which disrupt certain tertiary interactions in tRNA can also affect cleavage far away from the actual mutation. For example, a change from A9 to U9 affects cleavage at residues 36–38 in the anticodon loop. Similarly, a change from G10-C25 to C10-G25 leads to changes in the TΨC loop residues. These results suggest that structural alterations caused by the mutations in these folded regions of tertiary interaction can be propagated through the stacked nucleotides to affect structure at a distance.

Cleavage results with Rh(phen)$_2$phi^{3+} correlate well with lead cleavage data (Behlen et al., 1990) as shown in Table I. It seems that mutations which produced substantial effects on rhodium cleavage, in particular G46C and G10C-C25G, also showed large decreases in lead cleavage rates. In contrast, the A9U yielded only small changes in rhodium cleavage, yet large changes in lead cleavage. It should be noted, however, that there was a change in cleavage by the rhodium complex at U59 in this mutant. This may be significant since residue 59 is important for coordination by lead ion. In general, lead cleavage requires a high degree of stereochemical constraint and is therefore sensitive to local structure near the lead binding site. The rhodium complex is sensitive to local structural perturbations as well, and indeed, given that the complex binds at several sites on the polymer, the complex provides a probe for several different regions of the RNA. Furthermore, since the complex appears to probe tertiary interactions, perturbations at a distance from the binding sites which affect folding can also be sensitively assayed. Rhodium cleavage data on the tRNA^{Phe} mutants do not seem to correlate with the aminoacylation data. This is perhaps not surprising, however, since the rhodium complex does not seem to interact with regions of the tRNA which are important for making contacts with the tRNA synthetase (Sampson et al., 1989).

In conclusion, we have demonstrated on tRNA that cleavage by Rh(phen)$_2$phi^{3+} targets sites of tertiary interactions. The results obtained on yeast tRNA^{Asp} and the tRNA mutants indicate that cleavage patterns on yeast tRNA^{Phe} may reflect generally the recognition pattern of the complex for all tRNAs. Few and unique sites are cleaved in tRNAs, and the cleavage patterns observed vary sensitively with subtle changes in nucleic acid structure. Thus Rh(phen)$_2$phi^{3+} should provide a powerful probe in characterizing the folded structure of different tRNA mutants.

Might Rh(phen)$_2$phi^{3+} furthermore be valuable in characterizing other RNA structures? The complex appears to target

uniquely few sites within an RNA polymer. Regions which are double helical or single stranded are not preferentially bound. Furthermore, given the cleavage chemistry which involves no diffusible intermediate, the reaction is specific to the site of binding. Hence, cleavage patterns by the rhodium complex provide a sensitive and specific fingerprint to monitor structural changes in an RNA polymer as a function of different perturbations, substitutions, or reactions. On the basis of the tRNA cleavage data, it appears also that the complex is not specific for a single tertiary interaction. Sites cleaved by the rhodium complex mark a range of tertiary structures. Therefore, used in concert with other structural experiments, $Rh(phen)_2phi^{3+}$ may be a powerful and unique probe in characterizing the tertiary structures of other RNAs.

ACKNOWLEDGMENTS

We thank D. Moras for providing the purified yeast $tRNA^{Asp}$.

Registry No. $[Rh(phen)_2Phi^{3+}]$, 121174-96-7.

REFERENCES

Altman, S. (1984) *Cell 36*, 237–239.
Arnott, S., Hukins, D. W. L., Dover, S. D., Fuller, W., & Hodgson, A. R. (1973) *J. Mol. Biol. 81*, 107–122.
Barton, J. K. (1986) *Science 233*, 727–734.
Beardsley, K., Tao, T., & Cantor, C. R. (1970) *Biochemistry 9*, 3524–3532.
Behlen, L. S., Sampson, J. R., DiRenzo, A. B., & Uhlenbeck, O. C. (1990) *Biochemistry 29*, 2515–2523.
Cech, T. R. (1987) *Science 236*, 1532–1539.
Celander, D. W., & Cech, T. R. (1990) *Biochemistry 29*, 1355–1361.
Chow, C. S., & Barton, J. K. (1990) *J. Am. Chem. Soc. 112*, 2839–2841.
Chow, C. S., & Barton, J. K. (1991) *Methods Enzymol.* (in press).
Dock-Bregeon, A. C., Chevrier, B., Podjarny, A., Johnson, J., de Bear, J. S., Gough, G. R., Gilham, P. T., & Moras, D. (1989) *J. Mol. Biol. 209*, 459–474.
Ehresmann, C., Baudin, F., Mougel, M., Romby, P., Ebel, J. P., & Ehresmann, B. (1987) *Nucleic Acids Res. 15*, 9109–9128.
England, T. E., & Uhlenbeck, O. C. (1978) *Nature 275*, 560–561.
Garrett-Wheeler, E., Lockard, R. E., & Kumar, A. (1984) *Nucleic Acids Res. 12*, 3405–3422.
Guerrier-Takada, C., Lumelsky, N., & Altman, S. (1989) *Science 246*, 1578–1584.
Hall, K. B., Sampson, J. R., Uhlenbeck, O. C., & Redfield, A. G. (1989) *Biochemistry 28*, 5794–5801.
Huber, P. W., Morii, T., Mei, H.-Y., & Barton, J. K. (1991) *Proc. Natl. Acad. Sci. U.S.A.* (in press).
Kean, J. M., White, S. A., & Draper, D. E. (1985) *Biochemistry 24*, 5062–5070.
Kim, S. H., Sussman, J. L., Suddath, F. L., Quigley, G. J., McPherson, A., Wang, A. H., Seeman, N. C., & Rich, A. (1974) *Proc. Natl. Acad. Sci. U.S.A. 71*, 4970–4974.
Latham, J. A., & Cech, T. R. (1989) *Science 245*, 276–282.
Murakawa, G. J., Chen, C. B., Kuwabara, M. D., Nierlich, D. P., & Sigman, D. S. (1989) *Nucleic Acids Res. 17*, 5361–5375.
Patel, D. J., Shapiro, L., & Hare, D. (1987) *Q. Rev. Biophys. 20*, 78–90.
Peattie, D. A. (1979) *Proc. Natl. Acad. Sci. U.S.A. 76*, 1760–1764.
Pyle, A. M., & Barton, J. K. (1990) *Prog. Inorg. Chem. 38*, 413–475.
Pyle, A. M., Long, E. C., & Barton, J. K. (1989) *J. Am. Chem. Soc. 111*, 4520–4522.
Pyle, A. M., Morii, T., & Barton, J. K. (1990) *J. Am. Chem. Soc. 112*, 9432–9434.
Quigley, G. J., & Rich, A. (1976) *Science 194*, 796–806.
Romby, P., Moras, D., Bergdoll, M., Dumas, P., Vlassov, V. V., Westhof, E., Ebel, J. P., & Giege, R. (1985) *J. Mol. Biol. 184*, 455–471.
Romby, P., Moras, D., Dumas, P., Ebel, J. P., & Giege, R. (1987) *J. Mol. Biol. 195*, 193–204.
Rould, M. A., Perona, J. J., Söll, D., & Steitz, T. A. (1989) *Science 246*, 1135–1142.
Sampson, J. R., & Uhlenbeck, O. C. (1988) *Proc. Natl. Acad. Sci. U.S.A. 85*, 1033–1037.
Sampson, J. R., DiRenzo, A. B., Behlen, L. S., & Uhlenbeck, O. C. (1989) *Science 243*, 1363–1366.
Sampson, J. R., DiRenzo, A. B., Behlen, L. S., & Uhlenbeck, O. C. (1990) *Biochemistry 29*, 2523–2532.
Sitlani, A., Long, E. C., Pyle, A. M., & Barton, J. K. (1992) *J. Am. Chem. Soc.* (in press).
Werner, C., Krebs, B., Keith, G., & Dirheimer, G. (1976) *Biochim. Biophys. Acta 432*, 161–175.
Westhof, E., Dumas, P., & Moras, D. (1985) *J. Mol. Biol. 184*, 119–145.
Yanofsky, C. (1981) *Nature 289*, 751–758.